Taylor & Francis
Taylor & Francis Group

RESEARCH ARTICLE

 OPEN ACCESS Check for updates

Oral liposomal delivery of an activatable budesonide prodrug reduces colitis in experimental mice

Shiyun Xian[a,b†], Jiabin Zhu[c†], Yuchen Wang[a], Haihan Song[d] and Hangxiang Wang[a,b] (iD)

[a]The First Affiliated Hospital, National Health Commission (NHC) Key Laboratory of Combined Multi-Organ Transplantation, School of Medicine, Zhejiang University, Hangzhou, Zhejiang Province, P.R. China; [b]Jinan Microecological Biomedicine Shandong Laboratory, Jinan, Shandong Province, P.R. China; [c]Department of Pharmacy, The Obstetrics and Gynecology Hospital of Fudan University, Shanghai, P.R. China; [d]Central Lab, Shanghai Key Laboratory of Pathogenic Fungi Medical Testing, Shanghai Pudong New Area People's Hospital, Shanghai, P.R. China

ABSTRACT

Inflammatory bowel disease (IBD) is one of the most common intestinal disorders, with increasing global incidence and prevalence. Numerous therapeutic drugs are available but require intravenous administration and are associated with high toxicity and insufficient patient compliance. Here, an oral liposome that entraps the activatable corticosteroid anti-inflammatory budesonide was developed for efficacious and safe IBD therapy. The prodrug was produced via the ligation of budesonide with linoleic acid linked by a hydrolytic ester bond, which was further constrained into lipid constituents to form colloidal stable nanoliposomes (termed budsomes). Chemical modification with linoleic acid augmented the compatibility and miscibility of the resulting prodrug in lipid bilayers to provide protection from the harsh environment of the gastrointestinal tract, while liposomal nanoformulation enables preferential accumulation to inflamed vasculature. Hence, when delivered orally, budsomes exhibited high stability with low drug release in the stomach in the presence of ultra-acidic pH but released active budesonide after accumulation in inflamed intestinal tissues. Notably, oral administration of budsomes demonstrated favorable anti-colitis effect with only ~7% mouse body weight loss, whereas at least ~16% weight loss was observed in other treatment groups. Overall, budsomes exhibited higher therapeutic efficiency than free budesonide treatment and potently induced remission of acute colitis without any adverse side effects. These data suggest a new and reliable approach for improving the efficacy of budesonide. Our *in vivo* preclinical data demonstrate the safety and increased efficacy of the budsome platform for IBD treatment, further supporting clinical evaluation of this orally efficacious budesonide therapeutic.

1. Introduction

Inflammatory bowel diseases (IBDs), including Crohn's disease and ulcerative colitis, are recurrent and life-long inflammatory diseases of the gastrointestinal tract (Molodecky et al., 2012). Patients with IBDs suffer from abdominal pain, bloody diarrhea, anemia, and impaired quality of life; these diseases remain incurable and have emerged as a global public health challenge (Kaplan & Ng, 2017). Current recommended regimes adopted to manage IBDs include corticosteroids, sulfasalazine, immunosuppressants, antibiotics, and anti-tumor necrosis factor antibodies (De Vos et al., 1996; Lichtenstein et al., 2006; Kim JM et al., 2020). Most of these therapeutics require injection-based administration and repetitive dosing, which are associated with various adverse effects and low patient compliance, and many patients may face long-term medication (Lichtiger et al., 1994). Hence, developing expedient

formulations that are more efficacious and safe is essential for patients with recurrent and refractory IBDs.

Anti-inflammatory drugs, such as steroids, are widely used for clinical treatment of IBDs (Hanauer, 2002). Budesonide is a corticosteroid anti-inflammatory drug that was prioritized by the American Gastrointestinal Association as the 'first-choice' therapy for patients with IBDs with mild-to-moderate disease activity (Kozuch & Hanauer, 2008). Despite high activity as a topical agent, budesonide shows low systemic corticosteroid activity because of the rapid hepatic conversion to metabolites with negligible activities (Derendorf & Meltzer, 2008). Budesonide is poorly water-soluble and necessitates oral administration (Das et al., 2012). However, when orally administered, the low systemic bioavailability and high rate of liver clearance result in poor drug delivery to sites of intestinal inflammation and limit the efficacy (Labiris &

Dolovich, 2003). Therefore, strategies that enable high-efficiency and low-toxicity delivery will provide considerable benefit in expanding the clinical use of this potent drug (Thakor & Gambhir, 2013; Kim JH et al., 2019). In this regard, various delivery formulations have been developed. For instance, budesonide has been formulated into mesoporous silica microparticles for colon microbiota-triggered release (Ferri et al., 2019). In another tablet formulation, budesonide was entrapped in a polymer hydrogel to enable sustained release in the intestine (Herbada et al., 2021). However, preclinical studies in animal models have shown mixed success of these formulations compared with their free drug forms. To address this unmet medical challenge, it is preferable to rationally tailor chemical structures for a given agent to achieve favorable treatment outcomes.

Oral administration is a simple and painless approach for drug delivery and offers superior patient compliance and convenience, potentially improving disease outcomes compared with injection-based therapy (Kaur et al., 2019). To treat chronic IBDs, oral dosage forms of therapeutics could remarkably improve patient compliance and are regarded as an effective delivery system to improve local treatment efficacy across the gastrointestinal tract (Van den Mooter & Kinget, 1995; Vrettos et al., 2021; Xian et al., 2021). However, most currently adopted small-molecule drugs are poorly water-soluble and biopharmaceutics classification system (BCS) class II compounds (Narvekar et al., 2014; Tsume et al., 2014). Drugs with low solubility are difficult for the gastrointestinal tract to absorb, leading to poor bioavailability (Martinez & Amidon, 2002; Stegemann et al., 2007). In addition, the harsh conditions of the digestive tract impede effective drug accumulation at inflamed intestinal sites in an intact form (Lautenschläger et al., 2014; Liu et al., 2017). Thus, a method for the oral administration of BCS II pharmaceuticals could improve treatment outcomes for many diseases.

Extensive studies have demonstrated the potential of nanoparticle-based drug delivery to treat various diseases. Several nanotherapy formats have been approved for clinical use, and more have entered clinical trials (Caster et al., 2017). Among the various developed carriers, liposomes represent a mature, versatile platform with high capacity for the encapsulation of structurally dissimilar active compounds (Al-Jamal & Kostarelos, 2011). Drug-loaded liposomes have potential for clinical translation because of their high biocompatibility, low toxicity, and high loading efficiency for hydrophobic and hydrophilic drugs (Qiao et al., 2017). There have been notable successes in the clinical translation of liposomal formulations, including doxorubicin (Doxil®) (Barenholz, 2012) and irinotecan (Onivyde®) (Zhang, 2016). Compared with the free drug form, liposomal delivery improves therapeutic pharmacokinetics and pharmacodynamics (Silverman & Deitcher, 2013; He et al., 2019). To improve *in vivo* performance, the molecular structures of drug payloads can be rationally re-engineered using the prodrug strategy to enhance drug-carrier association (Wang H, Wu J et al., 2017). We previously demonstrated that the attachment of a structurally flexible polyunsaturated fatty acid (PUFA) augmented the avidity of a cytotoxic anticancer agent with delivery matrixes (Shi et al., 2020; Chen et al., 2022). Characterization of prodrug-loaded liposomes showed that compared with the burst release kinetics of free drugs, de novo engineered prodrugs had higher miscibility with the carriers and exhibited stimulus-triggered activation in a sustained and controllable manner. Therefore, this approach inhibits premature release of drug payloads at undesired sites but performs triggered release of chemically unmodified therapeutics at diseased lesions.

In this study, we present a synthetic budesonide derivative that is assembled into a liposomal nanovesicle (budsome), which is orally bioavailable for effective delivery to inflamed colon for IBD treatment. Our design rationale is based on the reversible ligation of budesonide to linoleic acid (LA) via an esterase-activatable linkage to generate the prodrug (**Figure 1**(a)). Owing to lipidation, the overall compound presented higher stability in the lipid bilayer than the parent budesonide molecule under the harsh conditions of the gastrointestinal tract but spontaneously released the active drug at the inflammatory site. Notably, orally administered budsomes outperformed free budesonide in both efficacy and safety in a preclinical mouse model of acute colitis. We believe that this activatable liposomal prodrug strategy developed by structure-guided design has substantial clinical potential for IBD treatment.

2. Materials and methods

2.1. Materials

Budesonide was purchased from TCI (Shanghai, China). LA was obtained from Macklin Biochemical Co., Ltd (Shanghai, China). Cholesterol, egg phosphatidylcholine (Egg-PC), and 1,2-distearoyl-*sn*-glycero-3-phosphoethanolamine-*N*-[methoxy (polyethylene glycol) 2000] (DSPE-PEG$_{2k}$) were purchased from A.V.T. Pharmaceutical Co., Ltd. (Shanghai, China).

2.2. Synthesis of the budesonide prodrug

The prodrug was synthesized via esterification in the presence of 1,3-diisopropylcarbodiimide (DISC) and 4-dimethylaminopyridine (DMAP). DISC (7.3 mg, 0.06 mmol) and DMAP (7.5 mg, 0.06 mmol) were added to a solution of budesonide (21.5 mg, 0.05 mmol) and LA (14.0 mg, 0.05 mmol) in 4 mL anhydrous dichloromethane (DCM) (Marquez Ruiz et al., 2013). The reaction mixture was refluxed overnight. After confirming the completion of the reaction, the crude product was washed with 5% citric acid, saturated NaHCO$_3$, and brine. The organic layer was dried over anhydrous Na$_2$SO$_4$, filtered, and evaporated under vacuum. The residue was further purified using flash column chromatography on silica gel (DCM:MeOH = 30:1) to yield the budesonide prodrug (23.0 mg, 71.4%). The chemical structure of final product was confirmed by ^{1}H nuclear magnetic resonance (NMR) spectroscopy, and the purity was validated by high-performance liquid chromatography (HPLC). HPLC was carried out on a Hitachi Chromaster system, and a YMC-Pack
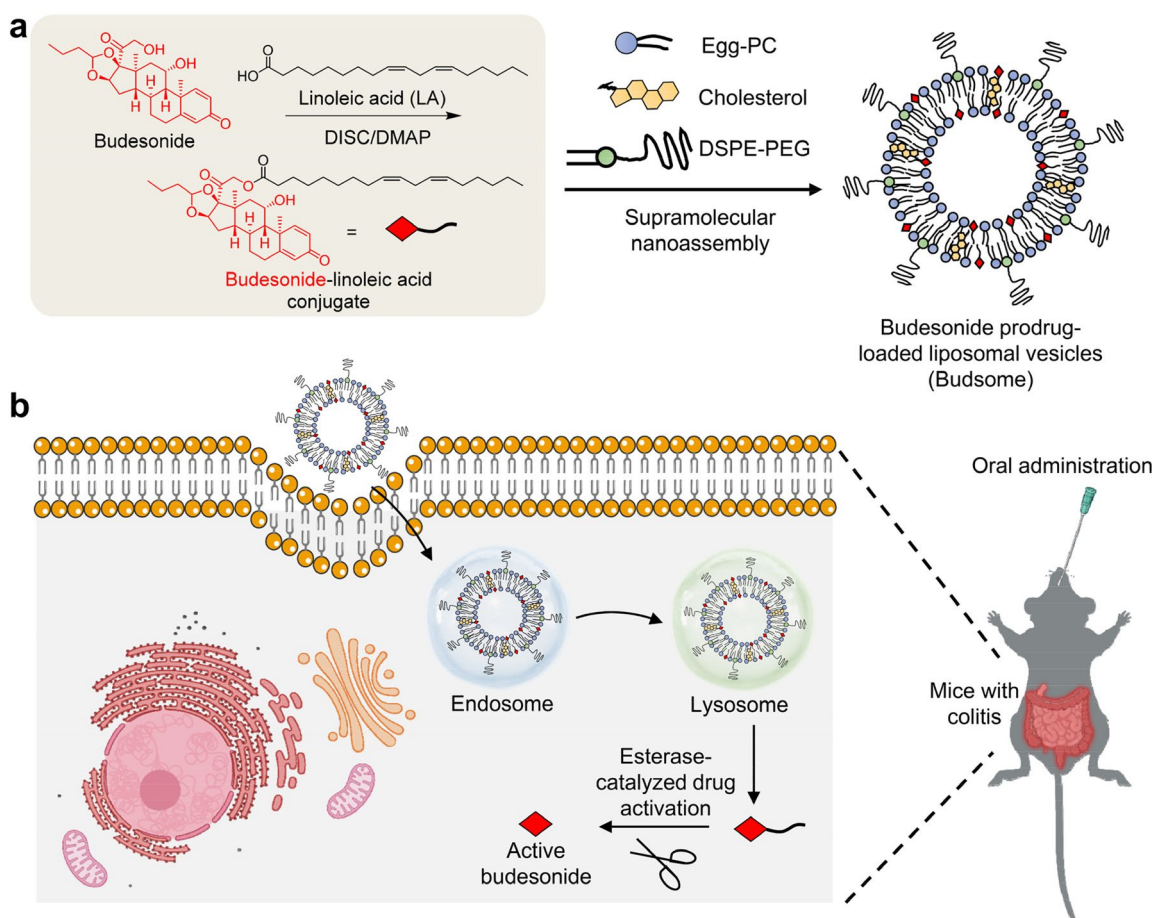
Figure 1. Budsome synthesis and formulation for IBD therapy. (a) Synthesis of the budesonide prodrug and nanoassembly of the prodrug with liposomal constituents to generate budsomes. (b) When administered orally, budsomes remain stable under the harsh conditions of the stomach, preventing the burst release of prodrug payloads. After preferential accumulation at the inflamed intestinal tissue in DSS-induced colitis mice, budsomes release biologically active budesonide.

C8 column (5 μm, 250 × 4.6 mm) at a flow rate of 1.0 mL/min. UV detection was performed at 220 nm. All runs used a linear gradient of 50–100% acetonitrile/water containing 0.1% TFA within 30 min.

2.3. Preparation of the budesonide prodrug-loaded liposomal nanoparticles (budsomes)

An ethanol dilution protocol as described in a previous report was used to prepare liposomes loaded with prodrug. First, Egg-PC, cholesterol, and DSPE-PEG$_{2k}$ were dissolved in 200 μL ethanol to obtain a lipid mixture at a mass ratio of 35:5:8. Next, the ethanolic solution was mixed with 20 μL dimethyl sulfoxide (DMSO) containing the prodrug (50 mg/mL, budesonide-equivalent) with a ratio of lipid to budesonide at 19:1 (wt/wt). The mixture was rapidly injected into deionized water to form liposomes (termed budsomes; 0.5 mg/mL, budesonide-equivalent). Liposome solutions were concentrated using ultracentrifugation (100,000 g, 20 min) and washed with deionized water to remove organic solvents (Shi et al., 2020). Liposomal nanoparticles encapsulating free budesonide (termed budesonide-LP) were also prepared according to the protocol described earlier.

2.4. Characterization of particle size

Hydrodynamic diameters (D_H) and distribution of budsomes (0.1 mg/mL, budesonide-equivalent) were determined using dynamic light scattering (DLS) with a Malvern Nano-ZS90 instrument (Malvern, UK) at 25 °C (Bhattacharjee, 2016). Each sample was measured three times.

2.5. Morphology analysis of budsomes

Transmission electron microscopy (TEM) was used to observe the morphology of budsomes. Budsome solution (0.1 mg/mL, budesonide-equivalent) was dropped onto a 300-mesh copper grid coated with carbon. After 2 min of deposition, the surface liquid was removed with filter paper and the deposit was subsequently stained with 2 wt% aqueous uranyl acetate solution for 1 min. Budsome morphology was observed using a Tecnai G2 spirit (Thermo FEI) at an acceleration voltage of 120 kV (Huang et al., 2021).

Budsome morphology was also characterized using cryo-electron microscopy (Cryo-EM) at the Center of Cryo-Electron Microscopy, Zhejiang University School of Medicine. An aliquot of 2.5 μL of the budsome solution (1.5 mg/mL, budesonide-equivalent) was deposited on a

glow-discharged holey carbon grid (Quantifoil Cu R1.2/1.3, 300 mesh), blotted for 5 s, and plunge-frozen in liquid ethane using a Vitrobot Mark IV (ThermoFisher Scientific)(Grassucci et al., 2007). Images were recorded with a Talos F200C equipped with a Ceta 4k × 4k camera.

2.6. Stability study

Budsome and budesonide-LP (0.1 mg/mL, budesonide-equivalent) were incubated with phosphate-buffered saline (PBS, pH 7.4), simulated gastric fluid (SGF, pH 1.2), and simulated intestinal fluid (SIF, pH 6.8). DLS was employed to investigate the stability of both formulations for seven consecutive days (Bhattacharjee, 2016).

2.7. Prodrug hydrolysis assay

In vitro hydrolysis of budesonide prodrug in the presence or absence of esterase was evaluated using high-performance liquid chromatography (HPLC). Briefly, the prodrug solution (0.2 mg/mL, budesonide-equivalent) was incubated with PBS containing 15 U/mL porcine liver esterase (PLE) in an orbital shaking water bath at 37 °C, and PBS without PLE was used as a control. Samples were collected at predetermined time intervals, and the amount of free budesonide hydrolyzed from the prodrug was analyzed via HPLC to investigate the esterase-responsive hydrolysis behavior. The same HPLC protocol was used to analyze free budesonide and the prodrug as described in the part of compound purity validation. The hydrolysis rate of the prodrug was calculated as a function of incubation time.

2.8. In vitro drug release

In vitro drug release in solutions of PBS, SGF, and SIF was evaluated using HPLC. Briefly, budsomes (0.2 mg/mL, budesonide-equivalent) were prepared according to the previous method. A total volume of 3 mL of budsomes was added to a dialysis bag of appropriate molecular weight and dialyzed against 15 mL of PBS containing 0.3% Tween 80. The dialysis bag was shaken continuously in a constant temperature water bath at 37 °C. Release solution (1 mL) was collected at predetermined time intervals and subsequently supplemented with an equal volume of fresh medium (Ren et al., 2022). Samples were analyzed using HPLC. *In vitro* drug release from budsomes was calculated as a function of incubation time. Drug release profiles in the presence of SGF or SIF were studied using a similar protocol.

2.9. In vivo distribution

Budsome *in vivo* distribution was evaluated in a dextran sulfate sodium (DSS)-induced colitis C57BL/6 mouse model using an IVIS Spectrum imaging system (Clairvivo OPT, Shimadzu Corporation, Kyoto, Japan). To induce inflammation of the intestinal tract, mice were fed water containing 3% DSS for seven consecutive days ($n=3$ in each group). Mice

with colitis are successfully established when they show bloody and dilute stools. Mice orally received free DiR (1,1'-dioctadecyl-3,3,3',3'-tetramethylindotricarbocyanine iodide, formulated in polysorbate 80/ethanol) and DiR-labeled budsomes at a DiR-equivalent dose of 1 mg/kg. At 6-h post-administration, mice were euthanized, and major organs including the heart, liver, spleen, lung, kidney, and colorectum were collected for *ex vivo* imaging. Subsequently, the colorectum was prepared in 8-μm frozen sections and stained with 4',6-diamidino-2-phenylindole (DAPI). DiR and DAPI signals were observed using confocal laser scanning microscopy (CLSM) (Han et al., 2019; Chung et al., 2020).

2.10. In vivo anti-inflammatory efficacy of budsomes

The *in vivo* anti-inflammatory efficacy of budsomes was assessed in C57BL/6 mice with colitis. Briefly, C57BL/6 mice were randomly divided into five groups and given 3% DSS in drinking water for 7 days ($n=6$/group) to establish an acute colitis mouse model (Han et al., 2019; Lee Y et al., 2020). Mice were orally administered free budesonide, the budesonide prodrug, or budsomes (0.2 mg/kg, budesonide-equivalent) on days 0, 1, 2, and 3. Free budesonide and the prodrug were both dissolved in Tween 80 and ethanol (1:1, vol/vol) and then diluted with saline. The severity of bloody diarrhea on day 6 was monitored using BASO fecal OB-II according to the manufacturer's protocol. The disease activity index (DAI), including body weight loss, stool consistency, and bleeding, was assessed on day 6 (Wang Y et al., 2021). On day 6 post-administration, mice were euthanized and their colons were excised and photographed.

2.11. Histological analysis of colon tissues

Histological analysis of colonic tissues was further examined using hematoxylin and eosin (H&E) and Masson's trichrome staining (Lee BC et al., 2020). Colons were preserved in formalin solution and embedded in paraffin. Tissue sections were then stained with hematoxylin for 5 min, followed by 2 s of differentiation in aqueous hydrochloric acid solution. Slides were then treated with aqueous ammonia solution for 15–30 s before being finally rinsed in distilled water. Subsequently, the sections were dehydrated in 95% alcohol and stained in eosin staining solution for 5–8 s. After sealing the slices with neutral gum, image acquisition and analysis were performed using CLSM.

Masson's trichrome staining was used to distinguish the collagen fibers in colon tissues (Mao et al., 2016). Briefly, paraffin-embedded colon tissues were sliced into sections, dewaxed with xylene, and rehydrated with graded alcohol. Sections were then stained with hematoxylin for 8 min followed by 10 min of staining in Biebrich scarlet-acid fuchsin solutions. Tissue sections were then treated with phosphotungstic/phosphomolybdic acid for 10 min and transferred directly into aniline blue for 5 min. After rinsing in dehydrating gradient ethanol and sealing the slices with neutral gum, the slices were examined under an optical microscope.

2.12. In vivo safety assessment of budsomes

In vivo safety of higher dose of budsomes was examined in healthy ICR mice. Healthy mice were randomly divided into three groups ($n=6$/group) and orally administered free budesonide or budsomes (2 mg/kg, budesonide-equivalent) every other day for 2 weeks. Another mouse group ($n=6$) that received an equal volume of saline was used as control. Mouse body weight was recorded every 2 days. On day 12, mice were euthanized and their major organs were collected, weighed, and H&E stained. In addition, critical blood parameters were determined using an animal hematology analyzer to evaluate the effect of budsomes on blood routine (Li et al., 2019).

2.13. Statistical analysis

Results are presented as mean ± SD. The statistical significance between measurements was examined using the unpaired Student's *t* test. $p < .05$ indicates statistical significance (*), $p < .01$ indicates high significance (**), and $p < .001$ indicates very high significance (***).

3. Results

3.1. Rational design and synthesis of the PUFAylated budesonide prodrug

PUFAs, such as LA, are excellent pro-moieties for the chemical derivatization of either hydrophobic or hydrophilic small-molecule therapeutics (e.g., cabazitaxel and 7-ethyl-10-hydroxycamptothecin). We previously showed that upon 'PUFAylation,' the resultant prodrug entities can self-assemble into water-dispersible nanostructures or co-assemble with exogenous excipients to form lipid nanoparticles (Wang H et al., 2015; Wang H, Lu et al., 2017; Fang et al., 2018; Wu et al., 2019; Xie et al., 2020; Chen et al., 2022). These therapeutic nanoparticles can be intravenously injected with improved tolerability and pharmacokinetics in animals. Budesonide, a 'first-choice' drug for treating mild-to-moderate ulcerative colitis, was chosen to generate an esterase-activatable prodrug in this study. As illustrated in Figure 1(a), LA was covalently tethered to the hydroxyl group of budesonide via an ester bond to generate the prodrug. The reaction readily proceeds in the presence of DISC/DMAP linkage chemistry with high yield. The final adduct was purified using silica gel chromatography and characterized using ^{1}H NMR spectroscopy (**Figure 2**(a,b)) and HPLC analysis (Figure 2(c,d)). The phenyl peaks from budesonide were clearly observed in the ^{1}H NMR spectrum at 6.02–7.28 ppm with characteristic double-bond peaks of LA at 5.30–5.42 ppm. Analytic HPLC also confirmed the sufficient purity of the conjugate and considerably increased affinity with the C8 column as evidenced by the increased retention time (Figure 2(d)). These results demonstrate the feasibility of producing the prodrug without using a tedious synthetic protocol, and we expected that the prodrug would have high miscibility with lipid matrixes.
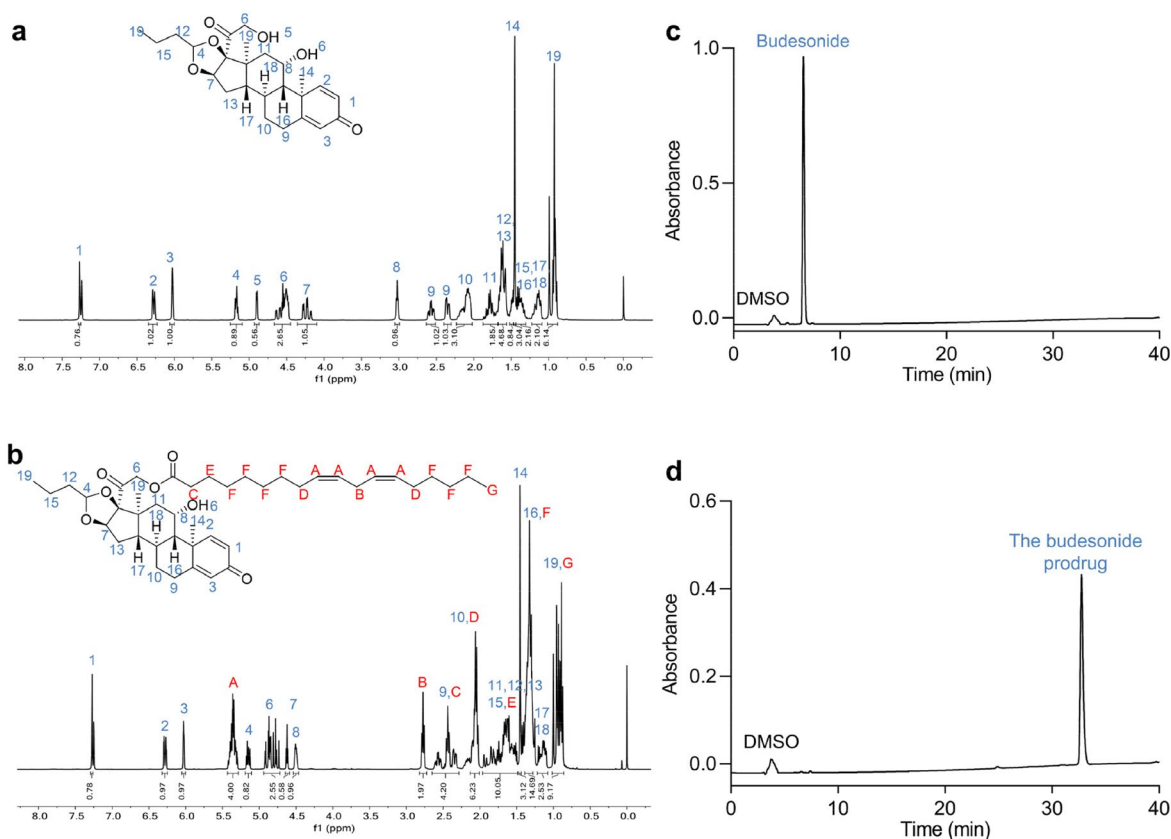

Figure 2. Structure confirmation and purity determination of the budesonide–LA conjugate. ^{1}H NMR spectra of budesonide (a) and the prodrug (b). HPLC confirmed the purity of budesonide (c) and the prodrug (d).

3.2. Liposomal formulation and nanoparticle characterization

Liposomes represent the most popular drug delivery carriers for clinical use. Currently, numerous liposomal formulations are available on the market, with more entering preclinical and clinical development. We therefore tested whether the prodrug can be supramolecularly assembled with lipid constituents to form liposomal vesicles (termed budsomes), which were prepared via an ethanol-injection method. In this protocol, the ethanol-dissolved lipid components, including Egg-PC, cholesterol, and DSPE-PEG$_{2k}$, were first mixed with the prodrug dissolved in DMSO. The mixture was then rapidly injected into stirred deionized water to form a uniform water-dispersible nanosuspension. Finally, the budsomes were purified via ultracentrifugation and washed with deionized water to remove organic solvents.

The liposomal formulation was subsequently characterized. As shown in **Figure 3**(a), DLS determined that the hydrodynamic diameter (D_H) of the budsomes was ~150 nm with a polydispersity index (PDI) of 0.234. TEM imaging showed that the prepared budsomes had a spherical shape ~100 nm in diameter (Figure 3(b)). The budsome size from the TEM

images was smaller than that from the DLS results as the samples used for TEM were processed in a dry state on carbon-coated copper grids, whereas the DLS samples were prepared in solution. Cryo-EM observation clearly revealed the presence of typical liposomal structures with a characteristic lipid bilayer (Figure 3(c)). Further analysis of Cryo-EM images indicated that the particle size of liposomes was ~151.70 ± 42.03 nm, which was consistent with the hydrated particle size measured using DLS.

Oral administration is regarded to be more convenient and acceptable than injection-based medication for treating IBDs. However, orally administered therapeutics must be stable to acid- and protease-catalyzed degradation to reach the sites of intestinal inflammation. To simulate the environment faced by delivery in the gastrointestinal tract, we used solutions such as SGF (pH 1.2) and SIF (pH 6.8) to investigate budsome stability. Unmodified budesonide-loaded liposomes (budesonide-LP) were also prepared for comparison. DLS measurements showed that budsomes had favorable colloidal stability in all tested media (PBS, SGF, and SIF), with negligible variations in D_H and PDI within 1 week (Figure 3(d–f)). In contrast, budesonide-LP exhibited greater distribution in
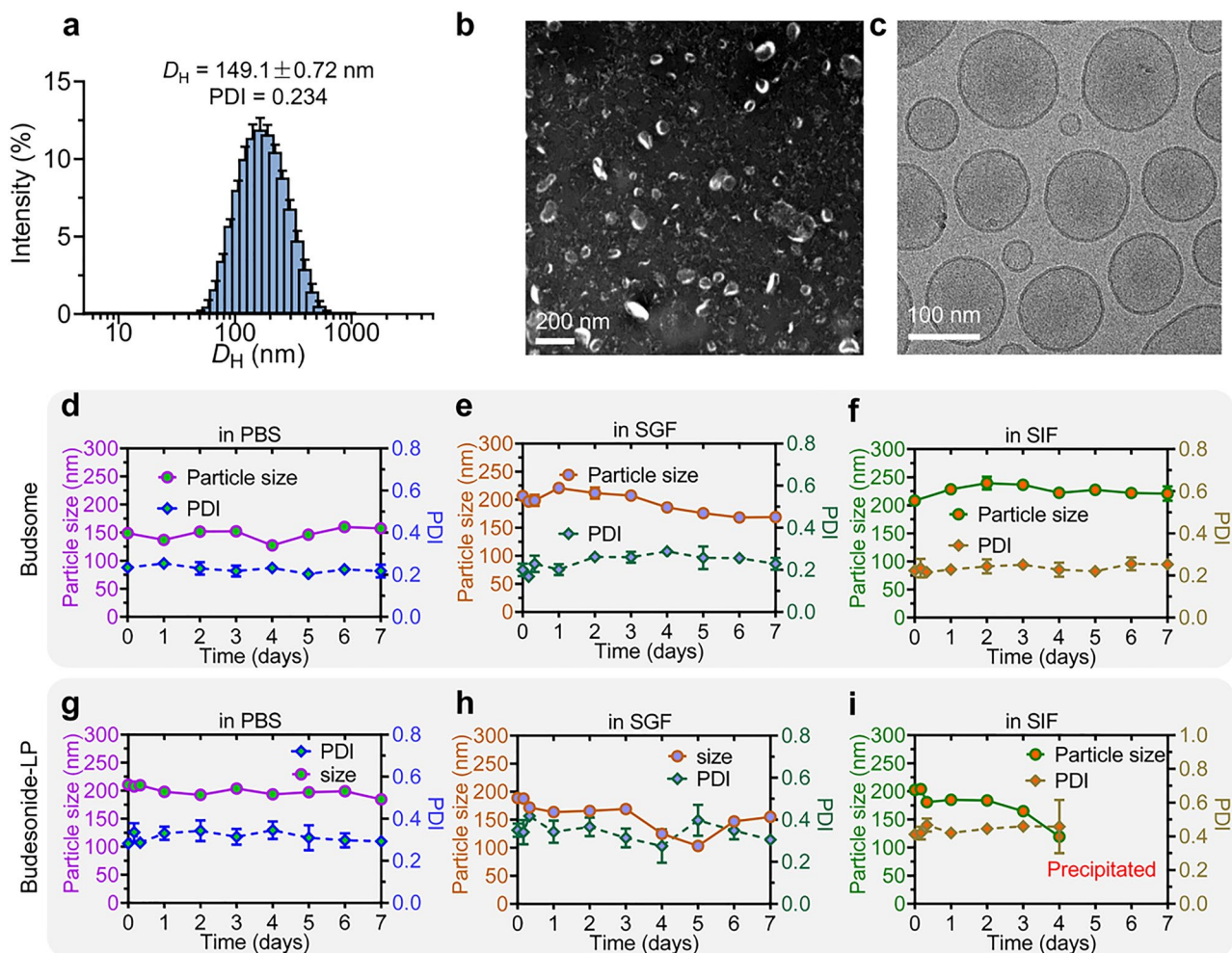

Figure 3. Budsome characterization. (a) Size distribution and D_H of budsome formulation measured using DLS. (b) TEM image of budsomes. Scale bar: 200 nm. (c) Cryo-EM image. Scale bar: 100 nm. (d–f) Colloidal stability of budsomes over 7 days at 37 °C. Free budesonide was also loaded into the liposomes (budesonide-LP) with the same lipid constituents. Budsome stability in (d) PBS, (e) SGF (pH 1.2), and (f) SIF (pH 6.8). Budesonide-LP stability in (g) PBS, (h) SGF, and (i) SIF. Data were determined by changes in particle size and PDI and are presented as mean ± SD ($n = 3$).

particle size in PBS than seen with budsomes. We also observed that budesonide-LP was insufficiently stabile under harsh conditions upon short-term incubation (Figure 3(g–i)). These comparative studies suggest that tailoring the molecular structures of drugs using the prodrug strategy can be leveraged to enhance drug-carrier association, thereby augmenting the overall inertness and protecting the budsomes from degradation in the harsh gastrointestinal tract.

3.3. Drug activation kinetics

The ester bond is susceptible to esterase-catalyzed hydrolysis in cells, thereby enabling *in situ* release of chemically unmodified budesonide for therapeutic activity. To verify whether active budesonide can be released in response to esterase activity, we examined the hydrolysis of the prodrug against PBS in the presence and absence of esterase using HPLC. The prodrug was almost completely converted to the active form within 48 h of incubation with PLE (15 U/mL) (**Figure 4**(a)). In contrast, under the esterase-free condition, the ester bond remained intact and negligible hydrolysis of the prodrug was observed. This result suggests that PUFAylation via the ester bond shields the pharmacological efficacy of the prototype drug, enabling it to be *in vivo* transported intact and inert while regaining activity in target cells upon esterase-based hydrolysis.

To further evaluate release and activation under digestive conditions that mimic the gastrointestinal tract, the behavior of budsomes was assessed via dialysis against PBS, SGF, or SIF. Interestingly, in acidic SGF medium, a very slow-release rate was observed, with only 5% of total drug liberated from the liposomal bilayer within 6 h (Figure 4(b)). Conversely, when budsomes were dialyzed against SIF or PBS at neutral pH, drug molecules tended to be released more quickly from the nanocarriers (Figure 4(c,d)). This could be attributed to the ease of cleavage of the ester bond with mild alkaline treatment. The retention time of orally administered drugs in the stomach is only 6 h. Thus, these results imply that orally delivered budsomes present satisfactory resistance in a gastric acid environment of pH 1.5 while spontaneously releasing drug payloads in an intestinal environment of pH 6.8.

3.4. Budsomes preferentially adhere to and accumulate in inflamed colon

Inflammatory intestines are characterized by leaky vascular structures (Haep et al., 2015). Nanosized therapeutic particles with anionic surface charges are envisioned to be adhesive to cationic inflamed surfaces at diseased lesions following oral administration (Jubeh et al., 2006; Xiu et al., 2020). We therefore analyzed the biodistribution of budsomes to test this hypothesis in an acute colitis model. Acute intestinal inflammation in C57BL/6 mice was induced *via ad libitum* administration of 3% DSS in drinking water for 7 days (**Figure 5**(a)). We labeled the budsomes with the near-infrared (NIR) dye DiR to track *in vivo* distribution and administered the nanoparticle solution to the mice with acute colitis *via* oral gavage; healthy mice were also included for comparison. At 6-h post-administration, animals were euthanized and major organs were excised for *ex vivo* fluorescence imaging (excitation wavelength: 750 nm, emission wavelength: 782 nm). The fluorescence signals derived from DiR-labeled budsomes primarily accumulated in inflamed colons, whereas only a low level of fluorescence was seen in other organs (Figure 5(b)). In addition, healthy mice treated with budsomes exhibited negligible fluorescence signals in the colon, indicating that liposomes could not penetrate the healthy colon because
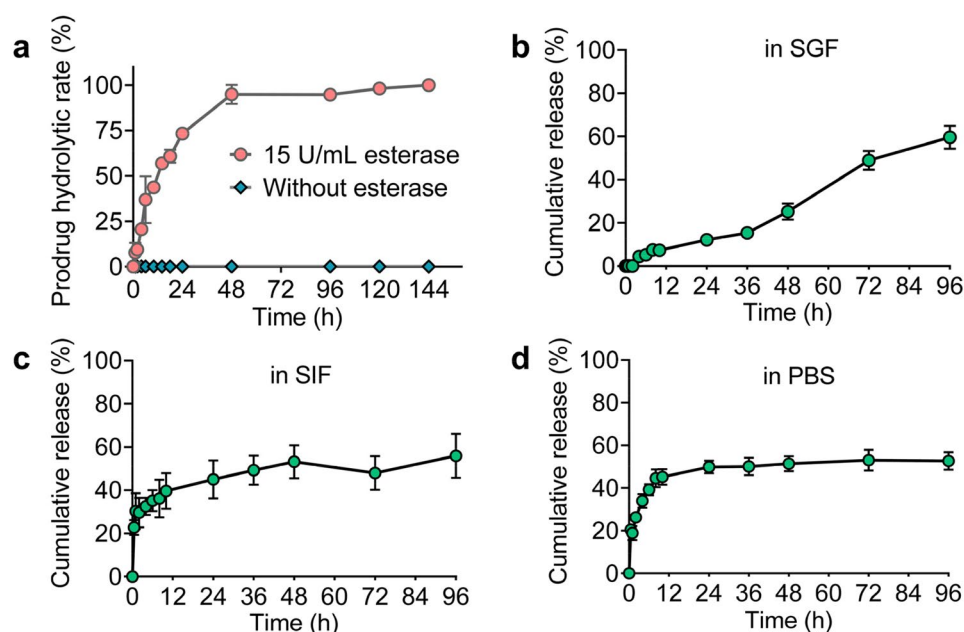

Figure 4. Esterase-catalyzed drug activation and drug release from budsomes. (a) Prodrug hydrolysis rate of the budesonide prodrug was determined at 37 °C against PBS with or without PLE (15 U/mL). *In vitro* cumulative release of drugs from budsomes in PBS (b), SGF (c), and SIF (d) monitored by HPLC. Data are presented as mean ± SD (*n* = 3).
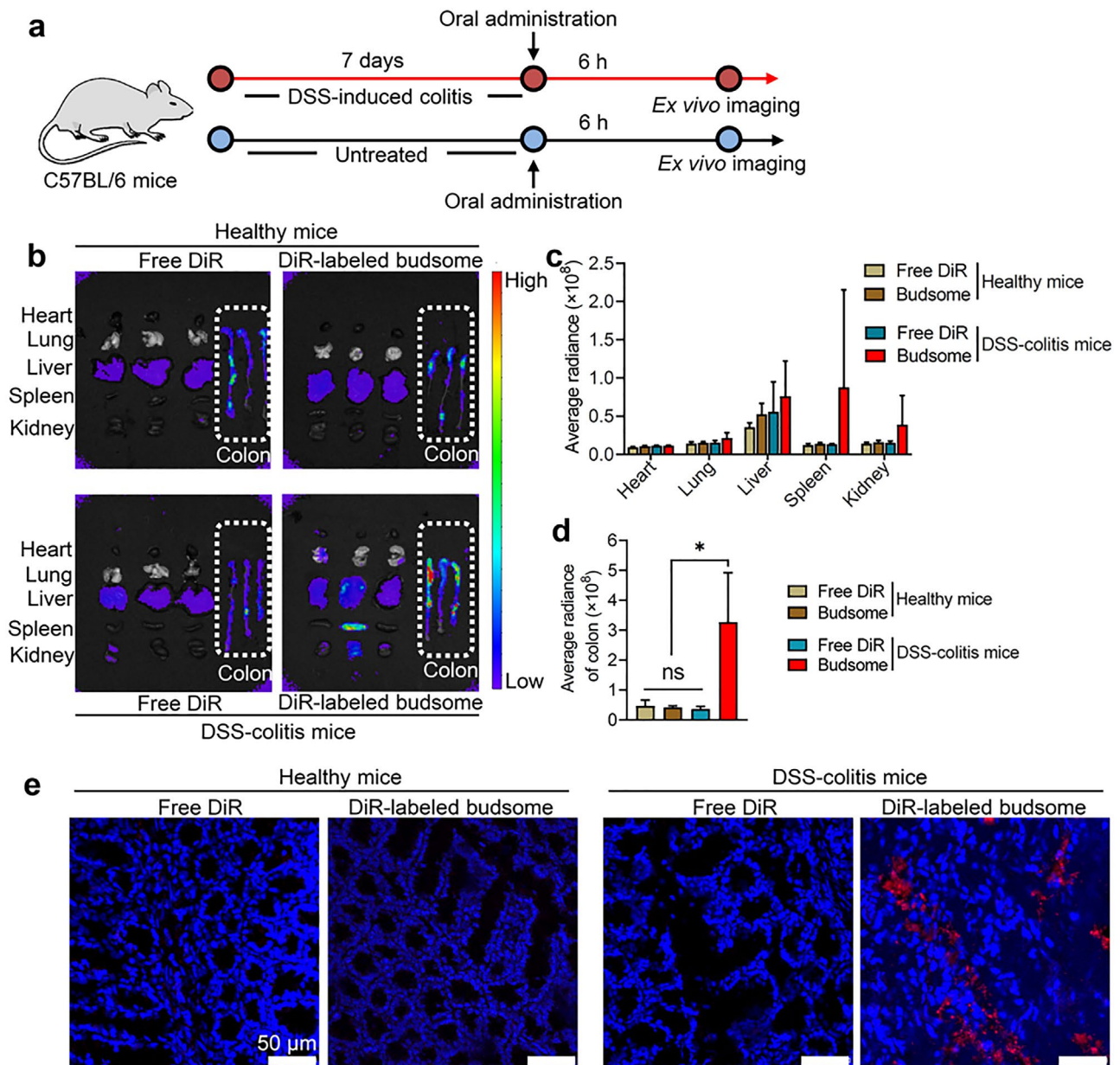
Figure 5. Analysis of nanoparticle accumulation in inflamed colons. (a) Experimental protocol for the establishment of an acute colitis model in mice and nanoparticle treatment. (b) NIR fluorescence intensity of excised major organs (heart, liver, spleen, lung, kidney, and colon) at 6 h post-administration. *In vivo* real-time distribution of budsomes was tracked in C57BL/6 mice after oral administration of DiR-labeled budsomes or free DiR. Average fluorescence intensity of each (c) organ and (d) colon. (e) Representative fluorescence images of colon sections visualized using CLSM at 6-h post-treatment. Data are presented as mean ± SD (*n* = 3). *p < .05, **p < .01, ***p < .001.

of the tight epithelial junctions. In contrast, orally administered free DiR had much lower NIR fluorescence signals than that of budsomes in either the colitis model or healthy mice, presumably because of their rapid clearance from the body following treatment. Quantification of fluorescence intensity also confirmed that the budsomes had favorable adhesion (~3 times) to the inflamed epithelium compared with that of either free DiR or in healthy colons (Figure 5(c,d)). Colon tissue slices were further examined using CLSM. DiR-derived signals penetrated throughout the tissues after oral administration of budsomes, whereas almost no fluorescence signals were detected in free DiR-treated or healthy mouse colons (Figure 5(e)).

3.5. Oral budsome treatment effectively ameliorates DSS-induced acute colitis in mice

The DSS-induced colitis murine model is the most widely used colitis model in experimental animals. DSS-colitis mice present intestinal inflammation, epithelial barrier function loss, dysregulated host innate immunity, and severe bleeding, which are similar to the clinical and pathological features of human IBDs. We established an acute colitis model in C57BL/6 mice to further evaluate the therapeutic efficacy of orally administered budsome. Healthy mice (~20 g in weight) were orally given 3% DSS in drinking water to develop acute intestinal colitis (**Figure 6**(a), see the experimental protocol). Following successive DSS administration, severe watery
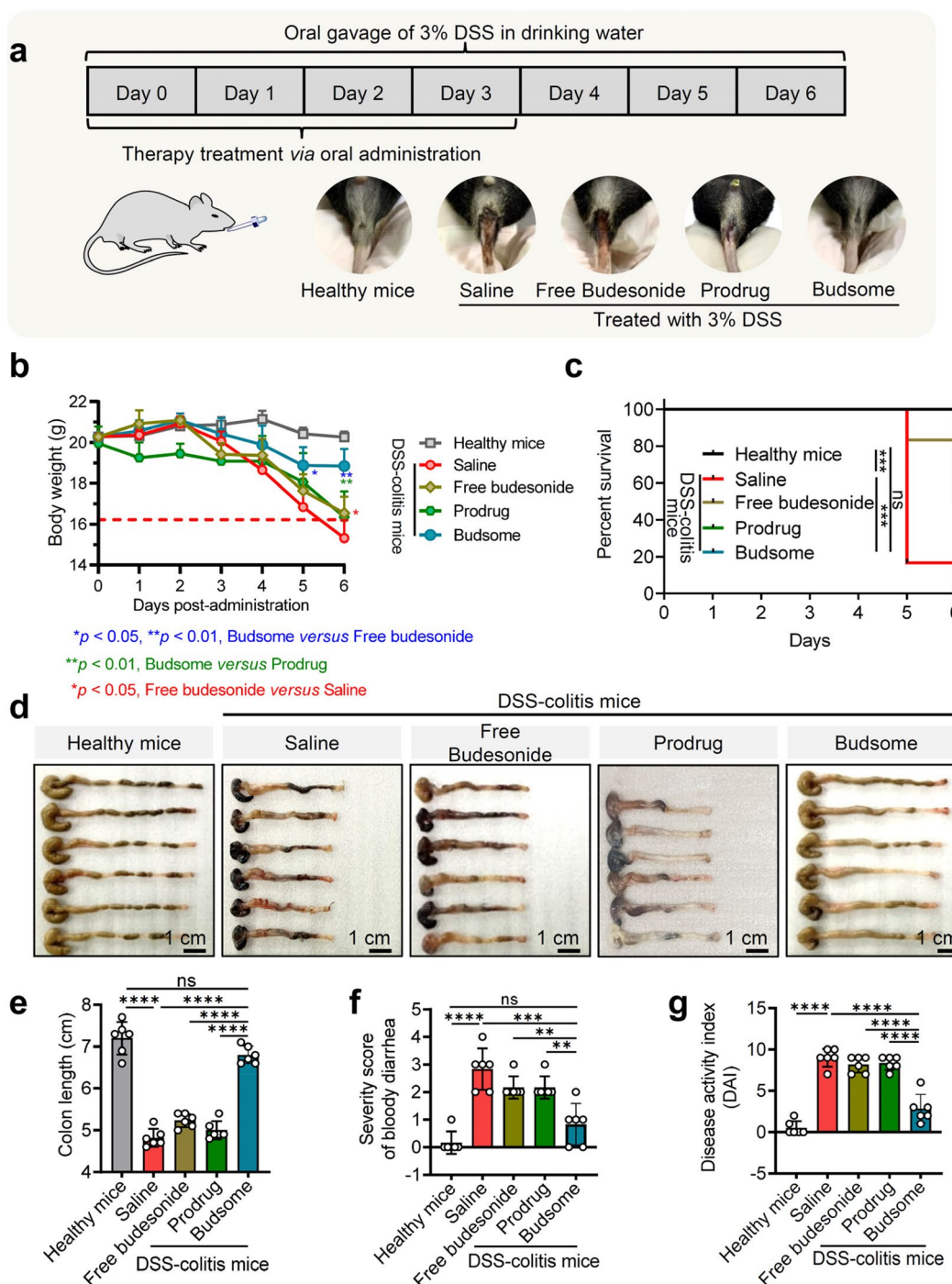
Figure 6. Budsomes ameliorate DSS-induced acute colitis in mice. (a) Schematic of the DSS-induced colitis model in C57BL/6 mice. (b) Weight changes. (c) Kaplan–Meier survival curves compared using the log-rank test. Photographs of (d) excised colons and (e) colon lengths measured at the end-point of the study. (f) Severity of bloody diarrhea and (g) DAI. Data are presented as mean ± SD ($n = 6$). *$p < .05$, **$p < .01$, ***$p < .001$.

diarrhea, rectal bleeding, and rectal prolapse were observed in the mice; however, oral treatment with budsomes allayed these clinical manifestations in DSS-colitis mice (Figure 6(a)). Animals with acute colitis also showed substantial body weight loss (i.e. the average loss was ~24%) and 100% mortality at the end-point of the study (weight loss of 20% defined as death) (Figure 6(b,c)). Unfortunately, oral gavage of free budesonide at 0.2 mg/kg only showed limited effect in inhibiting the reduction of mouse body weight with

average ~18% weight loss, and half of the mice died. On the other hand, mice treated with the budesonide prodrug also suffered from aggressive colitis with dramatic drop of their body weight (~16%) and half of mice died. Impressively, budsome treatment did protect against DSS-induced body weight loss (~7% weight loss) and improve the survival rate (Figure 6(b,c)), indicating the potency of budsomes to prevent colitis onset. Inflammation generally induces shortening of the colon length in this colitis mouse model. Strikingly, we
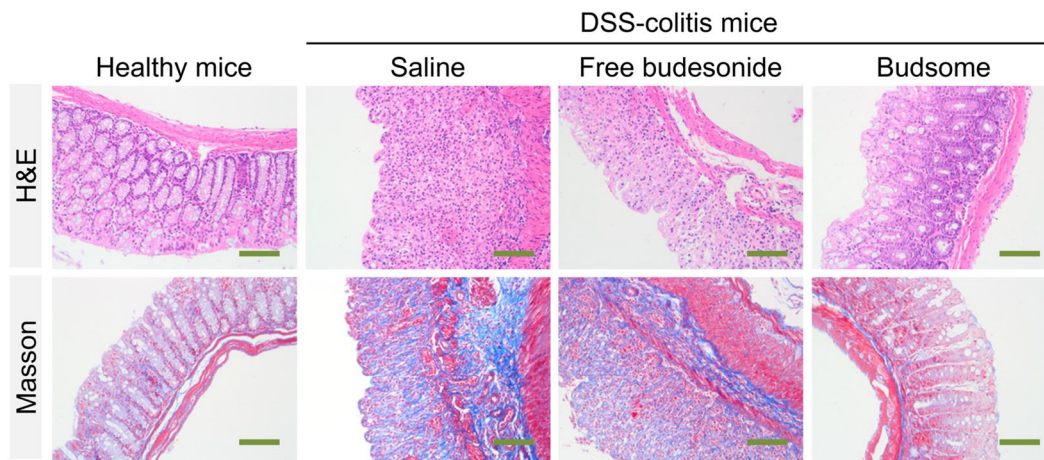
Figure 7. Representative images of colon sections stained with H&E and Masson's trichrome. Scale bars: 100 μm.
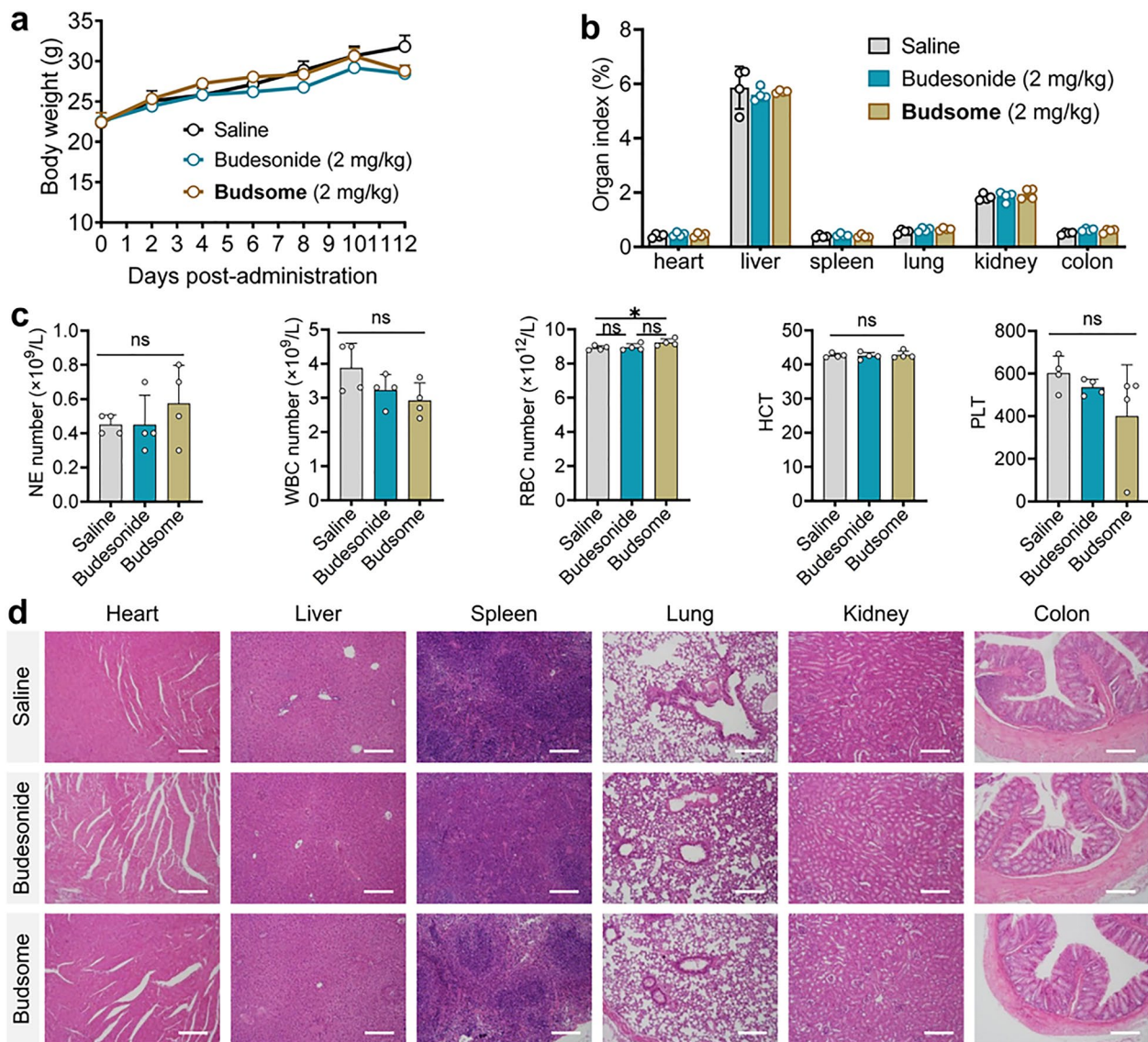

Figure 8. Comparative toxicity assessment of budsomes versus free budesonide in ICR mice. (a) Body weight change of mice in each treatment group. Healthy mice were orally administered budsomes or free budesonide at 2 mg/kg budesonide-equivalent dose (10-fold the therapeutic dose) every 2 days to examine *in vivo* toxicity. (b) Mice were euthanized at the end-point of the study, and major organs were collected and weighed. (c) Hematology parameters on day 12 after oral gavage (neutrophils, NE; white blood cells, WBC; red blood cells, RBC; hematocrit, HCT; and platelets, PLT). (d) Tissue histology from mice with different treatments. Scale bars: 50 μm. Data are presented as mean ± SD ($n = 6$). *$p < .05$, **$p < .01$, ***$p < .001$.

found that treatment with budsomes potently preserved colon length, whereas treatment either with free budesonide or the prodrug was almost ineffective (Figure 6(d,e)). For example, the colon length in budsome-treated mice was 6.8 ± 0.21 cm, which was similar to that of healthy mice ($p > .05$, budsome treatment vs. healthy mice); however, the colons of the mice after treated with free budesonide and the prodrug were all less than 5.5 cm in length.

Bloody diarrhea is a parameter reflecting the progression of acute enteritis, and higher scores measured by BASO fecal OB-II corresponded with increased symptom severity. DSS-colitis mice had severe bloody stools, with stool occult blood scores >2. Encouragingly, budsome treatment significantly reduced bloody diarrhea and relieved the malignant progression of IBDs (Figure 6(f)). Free budesonide and the prodrug therapy failed to reduce colitis potently. Furthermore, we evaluated the DAI using a 0–4 scoring system for the following parameters: stool consistency, bloody stool, and weight loss (scoring scheme). Budsome-treated mice exhibited lower DAI scores (Figure 6(g)). In contrast, most mice receiving free budesonide and the budesonide prodrug exhibited hair disorder, apathy, loose stools, and bloody stools, suggesting minimum therapeutic effect of clinically approved budesonide when orally delivered.

Histological analyses, including H&E staining and Masson's trichrome staining, were performed to estimate the anti-inflammatory efficacy of budsome treatment. Representative H&E staining images revealed significantly reduced inflammation in mice receiving budsome treatment (***Figure 7***). In contrast, histological damage such as impaired integrity of the mucosal epithelium, decreased villi height and crypt depth, interstitial edema, and inflammatory infiltration were observed in saline-treated or free budesonide-treated (0.2 mg/kg) mouse colons. Furthermore, representative images of Masson's staining showed the presence of pathologically excessive fibrotic tissues in the colon of DSS-colitis mice after treatment with saline or free budesonide, suggesting aggressive progression of acute inflammation. In sharp contrast, the epithelial damage and generation of fibrotic tissues were significantly reduced after treatment with budsomes, showing similar morphology with the colons of healthy mice.

3.6. Safety evaluation of budsomes in animals

Finally, healthy ICR mice were used to evaluate the safety of the budesonide prodrug delivered in liposomes. Mice were treated with free budesonide or budsomes at a high dose that was 10-fold above the therapeutic dose (2 mg/kg, budesonide-equivalent) via oral gavage to evaluate the biosafety. Mouse body weight was monitored throughout the experiment, and main organs (heart, liver, spleen, lung, kidney, and colon) were excised for further analysis on the last day. Neither free budesonide nor budsome treatment caused abnormalities in body or organ weights (***Figure 8***(a,b)). Hematologic parameters of blood samples were further measured after the last dose. Except for a slight change in the number of red blood cells, the hematologic parameters

(neutrophils, white blood cells, hematocrit, and platelets) fluctuated within normal ranges (Figure 8(c)). Histological analyses of major organs were performed to examine the damage induced by drugs. No significant histological changes were observed in mice treated with the liposomal drugs at a high dose (Figure 8(d)). These results suggest that budsomes can be safely administered via oral gavage.

4. Discussion

IBDs are inflammatory disorders of the intestinal tract and are typically recurrent and persistent (Yantiss & Odze, 2006). One consequence of chronic IBDs is tumorigenesis, and a considerable number of patients with IBD have a high risk of developing colitis-associated colorectal cancer (Saleh & Trinchieri, 2011). Currently, budesonide is a frontline steroid therapy that outperforms other common steroids; however, budesonide has low bioavailability and undergoes extensive first-pass liver metabolism when taken orally (McKeage & Goa, 2002; Fedorak & Bistritz, 2005). This has led to the development of more effective and less toxic therapeutics to address this clinical challenge, which could also favor the long-term medication for patients with IBDs. Orally administered therapeutics inevitably face the problems of low bioavailability and inefficient delivery (Ting et al., 2014). Rational nanoformulation approaches could provide a promising method to prevent active therapeutics from degrading in the gastrointestinal tract (Shahbazi & Santos, 2013). IBDs can cause breakdown in intestinal barrier function and pathological increase in intestinal permeability (Chelakkot et al., 2018; Scott et al., 2020). Therefore, orally administered nanosystems are expected to possess physiological tropism toward inflamed vasculature and preferentially accumulate in inflamed intestinal tissues owing to their high permeability and retention. As expected, we found that budsomes tended to accumulate in inflamed colons and the results of CLSM observation consistently demonstrate that the accumulation of the prodrug was significantly increased in the inflamed colons of DSS-colitis mice.

By rendering drugs temporarily inactive via a cleavable linkage, prodrug strategies can reasonably tailor the physicochemical properties of a given drug. For example, with re-engineered architectures, the avidity of prodrug entities to the delivery carriers can be augmented. Thus, these prodrugs can circulate in an intact and inert form but can then spontaneously activate at target sites upon enzymatic cleavage of the pro-moiety. We previously developed several such approaches to rationally reconstitute various types of small-molecule therapeutics. Drug PUFAylation using PUFAs as pro-moieties is of particular interest and has notable advantages: (i) this class of compounds is essential for biological functions and necessary for human nutrition, thus avoiding concerns over excipient-associated toxicity; (ii) they are commercially available for subsequent prodrug preparation; and (iii) covalent conjugation of PUFAs could increase association between prodrugs and delivery carriers, making the overall nanosystem sufficiently stable for storage and resistance against degradation after administration (Wu et al.,

2020). We therefore reversibly ligated clinically approved budesonide with the LA moiety and formulated this prodrug as pharmaceutically acceptable liposomal vesicles called budsomes for disease treatment. Upon oral administration, budsomes are colloidally stable in the stomach but release therapeutically active budesonide in response to high pH and esterase after approaching the inflamed colon.

DSS-induced colitis is the most widely used *in vivo* model, wherein a chemical irritant supplemented in drinking water causes epithelial erosion and inflammation in the colon within a short period, usually 4–5 days (Chassaing et al., 2014; Han et al., 2019). The pathological features of DSS-induced colitis in C57BL/6 mice are similar to those of human IBDs (Ito et al., 2008). Using this model, we tested the efficacy of the budsomes, orally administered four times, as a therapeutic regimen. In this clinically relevant colitis model, oral treatment with budsomes suppressed clinical indices and colonic inflammation scores, whereas free budesonide was less effective.

Although corticosteroids are effective therapy in patients with IBDs, they have severe systemic side effects (Lichtenstein et al., 2006). This toxicity must be taken into consideration during prodrug design as most patients with IBD face inevitable multiple repeat doses or even life-long medication in clinical management. Budsome therapy via oral administration was well tolerated. We found that a high dose of budsomes at 2 mg/kg (budesonide-equivalent), which was 10-fold greater than that of the therapeutic study, did not cause adverse side effects in animals. Covalent conjugation of budesonide could reduce undesired drug activation and leakage at unexpected sites. Moreover, the PUFA motif used for drug derivatization is nontoxic and a beneficial ingredient (Jacobson et al., 2008; Djuricic & Calder, 2021).

5. Conclusion

Oral administration represents the most convenient and cost-effective approach to deliver various therapeutics to diseased intestinal tissues for local anti-inflammatory therapy. Herein, we developed an orally deliverable liposomal vesicle that entrapped a budesonide prodrug for disease tissue-specific drug activation and pharmacology in a preclinical colitis mouse model. Our results demonstrated that a rationally chemically engineered prodrug can be stably encapsulated in liposomes to escort active drugs to lesion sites. The DSS-induced acute colitis mouse model demonstrated that oral budsome therapy significantly attenuated colonic inflammation without inducing dose-associated systemic toxicity. Although we have focused on budesonide here, it appears reasonable to anticipate that this approach would be applicable to other anti-inflammatory drugs. Therefore, we expect this budsome platform to exhibit high potential for further clinical translation.

Acknowledgments

Disclosure statement

Ethical approval statement

Funding

ORCID

Hangxiang Wang http://orcid.org/0000-0001-6370-9728

References

Al-Jamal WT, Kostarelos K. (2011). Liposomes: from a clinically established drug delivery system to a nanoparticle platform for theranostic nanomedicine. Acc Chem Res 44:1–14.

Barenholz YC. (2012). Doxil®—the first FDA-approved nano-drug: lessons learned. J Controlled Release 160:117–34.

Bhattacharjee S. (2016). DLS and zeta potential—what they are and what they are not? J Control Release 235:337–51.

Caster JM, Patel AN, Zhang T, Wang A. (2017). Investigational nanomedicines in 2016: a review of nanotherapeutics currently undergoing clinical trials. Wiley Interdiscip Rev Nanomed Nanobiotechnol 9:e1416.

Chassaing B, Aitken JD, Malleshappa M, Vijay-Kumar M. (2014). Dextran sulfate sodium (DSS)-induced colitis in mice. Curr Protoc Immunol 104:15.25.

Chelakkot C, Ghim J, Ryu SH. (2018). Mechanisms regulating intestinal barrier integrity and its pathological implications. Exp Mol Med 50:1–9.

Chen X, Cui L, Xu J, et al. (2022). De novo engineering of both an omega-3 fatty acid-derived nanocarrier host and a prodrug guest to potentiate drug efficacy against colorectal malignancies. Biomaterials 290:121814.

Chung CH, Jung W, Keum H, et al. (2020). Nanoparticles derived from the natural antioxidant rosmarinic acid ameliorate acute inflammatory bowel disease. ACS Nano 14:6887–96.

Das SK, Roy S, Kalimuthu Y, et al. (2012). Solid dispersions: an approach to enhance the bioavailability of poorly water-soluble drugs. Int J Pharmacol Pharm Technol 1:37–46.

De Vos M, Mielants H, Cuvelier C, et al. (1996). Long-term evolution of gut inflammation in patients with spondyloarthropathy. Gastroenterology 110:1696–703.

Derendorf H, Meltzer EO. (2008). Molecular and clinical pharmacology of intranasal corticosteroids: clinical and therapeutic implications. Allergy 63:1292–300.

Djuricic I, Calder PC. (2021). Beneficial outcomes of omega-6 and omega-3 polyunsaturated fatty acids on human health: an update for 2021. Nutrients 13:2421.

Fang T, Ye Z, Wu J, Wang H. (2018). Reprogramming axial ligands facilitates the self-assembly of a platinum(iv) prodrug: overcoming drug resistance and safer in vivo delivery of cisplatin. Chem Commun (Camb) 54:9167–70.

Fedorak RN, Bistritz L. (2005). Targeted delivery, safety, and efficacy of oral enteric-coated formulations of budesonide. Adv Drug Deliv Rev 57:303–16.

Ferri D, Costero AM, Gavina P, et al. (2019). Efficacy of budesonide-loaded mesoporous silica microparticles capped with a bulky azo derivative in rats with TNBS-induced colitis. Int J Pharm 561:93–101.

Grassucci RA, Taylor DJ, Frank J. (2007). Preparation of macromolecular complexes for cryo-electron microscopy. Nat Protoc 2:3239–46.

Haep L, Britzen-Laurent N, Weber TG, et al. (2015). Interferon gamma counteracts the angiogenic switch and induces vascular permeability in dextran sulfate sodium colitis in mice. Inflamm Bowel Dis 21:2360–71.

Han W, Xie B, Li Y, et al. (2019). Orally deliverable nanotherapeutics for the synergistic treatment of colitis-associated colorectal cancer. Theranostics 9:7458–73.

Hanauer SB. (2002). New steroids for IBD: progress report. Gut 51:182–3.

He H, Yuan D, Wu Y, Cao Y. (2019). Pharmacokinetics and pharmacodynamics modeling and simulation systems to support the development and regulation of liposomal drugs. Pharmaceutics 11:110.

Herbada RS, Torres-Suárez AI, Otero-Espinar FJ, et al. (2021). Matrix tablets based on a novel poly (magnesium acrylate) hydrogel for the treatment of inflammatory bowel diseases. Int J Pharm 608:121121.

Huang L, Wan J, Wu H, et al. (2021). Quantitative self-assembly of photoactivatable small molecular prodrug cocktails for safe and potent cancer chemo-photodynamic therapy. Nano Today 36:101030.

Ito R, Kita M, Shin-Ya M, et al. (2008). Involvement of IL-17A in the pathogenesis of DSS-induced colitis in mice. Biochem Biophys Res Commun 377:12–6.

Jacobson JL, Jacobson SW, Muckle G, et al. (2008). Beneficial effects of a polyunsaturated fatty acid on infant development: evidence from the Inuit of Arctic Quebec. J Pediatr 152:356–64.

Jubeh TT, Nadler-Milbauer M, Barenholz Y, Rubinstein A. (2006). Local treatment of experimental colitis in the rat by negatively charged liposomes of catalase, TMN and SOD. J Drug Target 14:155–63.

Kaplan GG, Ng SC. (2017). Understanding and preventing the global increase of inflammatory bowel disease. Gastroenterology 152:313–21.e2.

Kaur G, Arora M, Kumar MR. (2019). Oral drug delivery technologies—a decade of developments. J Pharmacol Exp Ther 370:529–43.

Kim JH, Hong SS, Lee M, et al. (2019). Krill oil-incorporated liposomes as an effective nanovehicle to ameliorate the inflammatory responses of DSS-induced colitis. Int J Nanomedicine 14:8305–20.

Kim JM, Kim DH, Park HJ, et al. (2020). Nanocomposites-based targeted oral drug delivery systems with infliximab in a murine colitis model. J Nanobiotechnology 18:133.

Kozuch PL, Hanauer SB. (2008). Treatment of inflammatory bowel disease: a review of medical therapy. World J Gastroenterol 14:354–77.

Labiris NR, Dolovich MB. (2003). Pulmonary drug delivery. I. Physiological factors affecting therapeutic effectiveness of aerosolized medications. Br J Clin Pharmacol 56:588–99.

Lautenschläger C, Schmidt C, Fischer D, Stallmach A. (2014). Drug delivery strategies in the therapy of inflammatory bowel disease. Adv Drug Deliv Rev 71:58–76.

Lee BC, Lee JY, Kim J, et al. (2020). Graphene quantum dots as anti-inflammatory therapy for colitis. Sci Adv 6:eaaz2630.

Lee Y, Sugihara K, Gilliland MGIII, et al. (2020). Hyaluronic acid-bilirubin nanomedicine for targeted modulation of dysregulated intestinal barrier, microbiome and immune responses in colitis. Nat Mater 19:118–26.

Li S, Xie A, Li H, et al. (2019). A self-assembled, ROS-responsive Janus-prodrug for targeted therapy of inflammatory bowel disease. J Control Release 316:66–78.

Lichtenstein GR, Abreu MT, Cohen R, Tremaine W, American Gastroenterological Association (2006). American Gastroenterological Association Institute technical review on corticosteroids, immunomodulators, and infliximab in inflammatory bowel disease. Gastroenterology 130:940–87.

Lichtiger S, Present DH, Kornbluth A, et al. (1994). Cyclosporine in severe ulcerative colitis refractory to steroid therapy. N Engl J Med 330:1841–5.

Liu L, Yao W, Rao Y, et al. (2017). pH-Responsive carriers for oral drug delivery: challenges and opportunities of current platforms. Drug Deliv 24:569–81.

Mao H, Su P, Qiu W, et al. (2016). The use of Masson's trichrome staining, second harmonic imaging and two-photon excited fluorescence of collagen in distinguishing intestinal tuberculosis from Crohn's disease. Colorectal Dis 18:1172–8.

Marquez Ruiz JF, Kedziora K, Pigott M, et al. (2013). A nitrophenyl-based prodrug type for colorectal targeting of prednisolone, budesonide and celecoxib. Bioorg Med Chem Lett 23:1693–8.

Martinez MN, Amidon GL. (2002). A mechanistic approach to understanding the factors affecting drug absorption: a review of fundamentals. J Clin Pharmacol 42:620–43.

McKeage K, Goa KL. (2002). Budesonide (Entocort® EC capsules). Drugs 62:2263–82.

Molodecky NA, Soon IS, Rabi DM, et al. (2012). Increasing incidence and prevalence of the inflammatory bowel diseases with time, based on systematic review. Gastroenterology 142:46–54.

Narvekar M, Xue HY, Eoh JY, Wong HL. (2014). Nanocarrier for poorly water-soluble anticancer drugs—barriers of translation and solutions. AAPS Pharmscitech 15:822–33.

Qiao H, Fang D, Chen J, et al. (2017). Orally delivered polycurcumin responsive to bacterial reduction for targeted therapy of inflammatory bowel disease. Drug Deliv 24:233–42.

Ren L, Xu P, Yao J, et al. (2022). Targeting the mitochondria with pseudo-stealthy nanotaxanes to impair mitochondrial biogenesis for effective cancer treatment. ACS Nano 16:10242–59.

Saleh M, Trinchieri G. (2011). Innate immune mechanisms of colitis and colitis-associated colorectal cancer. Nat Rev Immunol 11:9–20.

Scott SA, Fu J, Chang PV. (2020). Microbial tryptophan metabolites regulate gut barrier function via the aryl hydrocarbon receptor. Proc Natl Acad Sci USA 117:19376–87.

Shahbazi M-A, Santos HA. (2013). Improving oral absorption via drug-loaded nanocarriers: absorption mechanisms, intestinal models and rational fabrication. Curr Drug Metab 14:28–56.

Shi L, Wang Y, Wang Q, et al. (2020). Transforming a toxic drug into an efficacious nanomedicine using a lipoprodrug strategy for the treatment of patient-derived melanoma xenografts. J Controlled Release 324:289–302.

Silverman JA, Deitcher SR. (2013). Marqibo®(vincristine sulfate liposome injection) improves the pharmacokinetics and pharmacodynamics of vincristine. Cancer Chemother Pharmacol 71:555–64.

Stegemann S, Leveiller F, Franchi D, et al. (2007). When poor solubility becomes an issue: from early stage to proof of concept. Eur J Pharm Sci 31:249–61.

Thakor AS, Gambhir SS. (2013). Nanooncology: the future of cancer diagnosis and therapy. CA: Cancer J Clin 63:395–418.

Ting Y, Jiang Y, Ho C-T, Huang Q. (2014). Common delivery systems for enhancing in vivo bioavailability and biological efficacy of nutraceuticals. J Funct Foods 7:112–28.

Tsume Y, Mudie DM, Langguth P, et al. (2014). The Biopharmaceutics Classification System: subclasses for in vivo predictive dissolution (IPD) methodology and IVIVC. Eur J Pharm Sci 57:152–63.

Van den Mooter G, Kinget R. (1995). Oral colon-specific drug delivery: a review. Drug Deliv 2:81–93.

Vrettos N-N, Roberts CJ, Zhu Z. (2021). Gastroretentive technologies in tandem with controlled-release strategies: a potent answer to oral drug bioavailability and patient compliance implications. Pharmaceutics 13:1591.

Wang H, Lu Z, Wang L, et al. (2017). New generation nanomedicines constructed from self-assembling small-molecule prodrugs alleviate cancer drug toxicity. Cancer Res 77:6963–74.

Wang H, Wu J, Xie K, et al. (2017). Precise engineering of prodrug cocktails into single polymeric nanoparticles for combination cancer therapy: extended and sequentially controllable drug release. ACS Appl Mater Interfaces 9:10567–76.

Wang H, Xie H, Wang J, et al. (2015). Self-assembling prodrugs by precise programming of molecular structures that contribute distinct stability, pharmacokinetics, and antitumor efficacy. Adv Funct Mater 25:4956–65.

Wang Y, Xie H, Ying K, et al. (2021). Tuning the efficacy of esterase-activatable prodrug nanoparticles for the treatment of colorectal malignancies. Biomaterials 270:120705.

Wu L, Zhang F, Chen X, et al. (2019). Self-assembled gemcitabine prodrug nanoparticles show enhanced efficacy against patient-derived pancreatic ductal adenocarcinoma. ACS Appl Mater Interfaces 12:3327–40.

Wu L, Zhang F, Chen X, et al. (2020). Self-assembled gemcitabine prodrug nanoparticles show enhanced efficacy against patient-derived pancreatic ductal adenocarcinoma. ACS Appl Mater Interfaces 12:3327–40.

Xian J, Zhong X, Gu H, et al. (2021). Colonic delivery of celastrol-loaded layer-by-layer liposomes with pectin/trimethylated chitosan coating to enhance its anti-ulcerative colitis effects. Pharmaceutics 13:2005

Xie H, Zhu H, Zhou K, et al. (2020). Target-oriented delivery of self-assembled immunosuppressant cocktails prolongs allogeneic orthotopic liver transplant survival. J Control Release 328:237–50.

Xiu Y, Wang K, Chen J, et al. (2020). Liposomal N-acylethanolamine-hydrolyzing acid amidase (NAAA) inhibitor F96 as a new therapy for colitis. RSC Adv 10:34197–202.

Yantiss R, Odze R. (2006). Diagnostic difficulties in inflammatory bowel disease pathology. Histopathology 48:116–32.

Zhang H. (2016). Onivyde for the therapy of multiple solid tumors. OncoTargets Ther 9:3001.